Part 1. Direct Measurement of Depletion Attraction and Thin Film Viscosity between Lipid Bilayers in Aqueous Polyethylene Glycol Solutions

Tonya L. Kuhl,*,† Alan D. Berman,† Sek Wen Hui,‡ and Jacob N. Israelachvili†

Department of Chemical Engineering, University of California, Santa Barbara, Santa Barbara, California 93106, and Department of Biophysics, Roswell Park Cancer Institute, Buffalo, New York 14263

Received September 29, 1997; Revised Manuscript Received July 1, 1998

ABSTRACT: Using the surface forces apparatus, we have measured the static and hydrodynamic forces between two substrate supported lipid bilayers in water and semidilute aqueous solutions of 8000 MW poly(ethylene glycol) (PEG), a neutral polymer for which water is a good solvent. At small separations ($D < R_F$, Flory radius), an enhanced adhesion due to depletion attraction was measured. Conversely, at larger separations we found a repulsive barrier, which is not predicted by mean-field theories. Dynamic measurements of the viscosity as a function of film thickness reflected the same pattern of behavior as exhibited in the static force experiments: Thus, in the absence of polymer, the shear plane was at the lipid-water interface, while in the 8000 MW polymer solution the viscosity *decreased* as a function of decreasing surface separation due to a polymer-depleted layer of lower viscosity at the bilayer surface. We discuss our results in terms of depletion attraction, depletion stabilization, thin film lubrication, the effective viscosity in thin films, and the possibility of polymer aggregates in PEG solutions. The crossover from depletion attraction to adsorption and repulsion with increasing MW is addressed in part 2 of this work.

Introduction

Asakura and Oosawa were the first to propose that the flocculation of particles in the presence of nonadsorbing macromolecules was due to a differential osmotic pressure setup once the macromolecules were excluded from the region between the particles.[1] Since then, a number of different theoretical treatises have addressed this phenomenon from a variety of viewpoints although the generally accepted explanation for depletion flocculation has remained unchanged.[2] In brief, an osmotic "depletion force" is expected to occur whenever nonadsorbing polymer is added to a colloidal dispersion. A polymer chain in solution will maintain, on average, that configuration that is entropically most favorable, i.e., a random coil in a good solvent. The coil may approach a surface to a distance such that its outermost segments just meet the surface. To approach more closely, the coil would have to adopt a less favorable conformation with a resulting loss of configurational entropy. Thus, a gradient in the polymer segmental concentration exists in the vicinity of a surface. Depletion attraction arises when the depletion layers, each of thickness Δ, associated with two surfaces overlap. Theoretically, at large separations, $D > 2\Delta$, the segment concentration increases from zero at the surface to that of the bulk solution in the middle of the gap between the surfaces. However, at smaller separations, $D < 2\Delta$, the concentration at the midplane falls below that of the bulk. As a result, the pressure in the bulk solution is greater than that in the gap, and there is an attractive osmotic force between the surfaces.

Although depletion *attraction* is widely accepted, the idea of depletion *stabilization* has remained ambiguous due to conflicting theoretical findings and a lack of direct experimental measurements. Neither simple scaling arguments nor mean-field descriptions of polymer solutions between surfaces predict a repulsion.[2] Conversely, Vincent et al.[3] have proposed that a restabilization of colloidal dispersions should occur at high polymer concentrations due to a decrease in the depletion layer thickness resulting in a weakened attraction, while Napper and Feigin[4] attribute depletion stabilization to a repulsive force due to the high energy cost of demixing the solution prior to the onset of the attractive regime. Walz and Sharma[5] have likewise predicted a repulsive barrier at separations between one and two diameters of the excluded macromolecule due to excluded volume effects when second-order interactions are taken into account. Similarly, recent work of Mao and co-workers[6] has also shown that excluded volume considerations can lead to a repulsive force regime between particles in semidilute concentrations of smaller nonadsorbing particles. When the excluded particles are rod shaped, the repulsive barrier is greatly enhanced, leading to kinetic stabilization. Ogden and Lewis have reported on one of the few experimental systems where a depletion stabilization interaction may be in effect.[32]

Direct experimental measurements of depletion attraction by Richetti and Kekicheff[7] due to the exclusion of cetyltrimethylammonium bromide (CTAB) micelles at high volume fractions were oscillatory, with the number of oscillations and their magnitude increasing with the micellar concentration as predicted by Walz and Sharma.[5] Similar measurements by Sober and Walz[8] using total internal reflection microscopy also detected depletion attraction in the presence of CTAB micelles. However, their micelle concentration was much lower than in the experiments conducted by Richetti and Kekicheff and no oscillations in the force were detected. Perez and Proust[9] measured a decrease in the repulsion between charged mica sheets immersed

† University of California, Santa Barbara.
‡ Roswell Park Cancer Institute.

10.1021/ma971431d CCC: $15.00
Published on Web 10/30/1998

in aqueous dextran solutions. They attributed the decrease in electrostatic repulsion between the charged surfaces to the possible presence of an attractive interaction due to the exclusion of dextran chains. However, the complexities of surface charge effects precluded a definite determination of a depletion interaction. Thus far, only ionic systems, which take advantage of a larger excluded volume effect, have been investigated since the depletion interaction or differential osmotic pressure becomes detectable at lower solute concentrations.

The experimental system studied here is a biologically relevant one of two lipid bilayers in aqueous solutions of poly(ethylene glycol). Classically, PEG has been used to aggregate and fuse biological colloids, i.e., vesicles, liposomes, and cells. Arnold et al.[10] proposed that the effect of PEG 8000 MW on membranes could be explained by depletion attraction based on the results of a series of experiments utilizing ESR, ^{2}H NMR, osmotic pressure, polarity, and dielectric constant. Because the experimentally measured ζ potentials in PEG solutions were less than expected, they suggested that PEG molecules were excluded from the bilayer surface. In contrast, when a short PEG chain (EO_8) was anchored to the vesicle surface by incorporation of octa(ethylene glycol) mono(*n*-dodecyl) ether ($C_{12}EO_8$) into the bilayer, a larger ζ potential was measured.[11] Evans and Needham[12] provided additional experimental proof of the depletion effect by micropipet aspiration measurements of dextran and PEG-enhanced adhesion of giant phospholipid vesicles and developed a self-consistent depletion force theory to explain the stronger adhesion measured in the presence of these nonadsorbing polymer. Moreover, their measured adhesion energies correlated extremely well with those expected from the measured osmotic pressures of the bulk polymer solutions.

We present direct and quantitative studies of the depletion phenomenon utilizing the surface forces apparatus technique (SFA). We measured both the static and dynamic normal forces between bilayer coated surfaces in semidilute, aqueous solutions of poly ethylene glycol of 8000 MW. In the presence of 8000 MW PEG an attractive depletion interaction was measured at small separations, $D < R_F$. We were particularly surprised to measure a repulsive barrier prior to the depletion attraction regime.[13] In light of the recent dynamic light scattering work of Porsch and Sundelöf,[14] where they determined that PEG itself does not aggregate in dilute water solutions but that any impurities in the solution quickly result in polymer aggregates, we also discuss whether polymer aggregates were the source of the long-range repulsion with 8000 MW PEG.

Experimental Section

Chemicals and Sample Preparation. Dimyristoyl phosphatidylcholine (DMPC) and dipalmitoyl phosphatidylethanolamine (DPPE) were purchased from Avanti Polar Lipids, Inc. (Alabaster, AL). PEG-8000 (8k) and potassium nitrate were from Sigma Chemical Co. (St. Louis, MO). All chemicals were used without further purification. PEG is water soluble at moderate temperatures in all proportions over a wide range of molecular weights (MWs).[15] The 0.02 μm aluminum matrix Anodisc filters were purchased from Whatman (England).

Traditionally, commercial grade 8k PEG is used to aggregate and fuse biological colloids. Although lower MWs can also be effective at very high concentrations, higher MWs are found to be ineffective. Thus, the behavior is very MW-dependent.

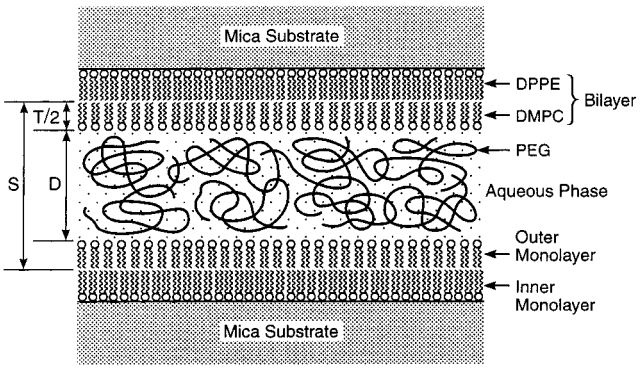

Figure 1. Schematic of the supported bilayer surfaces in an aqueous solution of 8000 MW PEG. The position of bilayer−bilayer contact, $D = 0$, was determined at the end of each experiment. First, the combined thickness of the two hydrated outer DMPC monolayers, *S*, was determined at the end of each experiment by measuring the thickness change following drainage of the solution from the apparatus, and removal of the two outer monolayers. Second, the anhydrous bilayer thickness, *T*, was calculated from the physical volumes occupied by the hydrocarbon chains and PC headgroups as given by $T = 2[2V_{hc} + V_{head}]/A$, where $V_{hc} = (27.4 + 26.9n)$ Å^3 is the average volume of a saturated *n*-carbon chain in the frozen or gel state,[19] $V_{head} = 324.5$ Å^3 is the average headgroup volume of PC,[20] and *A* is the deposited headgroup area.

Static Force Measurements. The apparatus used in the static surface force measurements has been described extensively.[16] Briefly, the technique enables the interaction forces, both attractive and repulsive, to be measured between two mica sheets, which are back-silvered and glued onto cylindrical silica disks. The separation between the mica surfaces is measured with an optical technique based on multiple beam interference fringes (fringes of equal chromatic order, FECO). From the wavelengths of the FECO fringes as measured in a spectrometer, the distance between the two surfaces is measured with a resolution up to 1 Å. The distance between the surfaces is controlled by a series of coarse and fine micrometers. Additional control of the separation is achieved with a piezoelectric crystal upon which the upper disk is mounted. The force between the surfaces is measured from the deflection of a double cantilever spring of stiffness *K* supporting the lower surface.

Bilayer surfaces, our model membranes, were constructed on the mica substrates using Langmuir−Blodgett deposition. The first or inner layer of the supported bilayer was DPPE (Π = 40 mN/m, 43 Å^2/molecule), which binds physically but strongly to the mica substrate. DMPC (Π = 31 mN/m, 58 Å^2/molecule) was deposited as the second or outer layer. DMPC was chosen because it is commonly used in PEG-induced aggregation and fusion experiments of vesicles.[17] After the DMPC layer was deposited, the disks were transferred under water to the measuring apparatus and mounted, as described elsewhere.[18] Prior to the insertion of the bilayer coated disks, the apparatus was filled with a degassed 0.5 mM KNO_3 water or PEG solution saturated with free DMPC to prevent lipid desorption from the bilayers during the experiments. A schematic of the bilayer-coated mica surfaces in PEG solution is shown in Figure 1.

Throughout this work, the surface separation, $D = 0$, was defined as contact between nominally dehydrated bilayers (cf. Figure 1). The position of bilayer−bilayer contact during experiments was of fundamental concern since a shift in this position is indicative of the interaction force being measured. In water, the supported bilayer surfaces adhere via van der Waals attraction at small separations ($D \approx 20$ Å), closer approach is opposed by strong hydration−steric protrusion repulsion (Figure 1). Thus, in the absence of polymer the hard wall of bilayer−bilayer contact occurs at $D \approx 20$ Å. In the case of polymer depletion attraction, the position of the hard wall of bilayer−bilayer contact should not change since no

polymer remains in the gap between the bilayers, while the adhesion force should scale with the bulk polymer concentration. In contrast, if the measured interaction is due to polymer bridging, the hard wall position is shifted outward to $D > 20$ Å by the adsorbed polymer layers trapped between the surfaces and the adhesion force no longer scales with the bulk osmotic pressure. Last, because the surfaces are coated with lipid bilayers, there is also the possibility of the measured force (especially an increase in the attraction and adhesion between the surfaces) to be the result of an increased hydrophobic interaction due to desorption of lipids from the bilayers exposing more hydrophobic groups. The desorption of lipids, however, would cause the position of contact to be closer in due to a less dense packing of the remaining lipids. Hence, both the position of bilayer−bilayer "contact" and the adhesion strength were used in this work to distinguish between the different types of forces operating between the bilayers.[22]

Viscosity Measurements. The same apparatus as used in static force measurements was used to measure the dynamic interaction of the two bilayers immersed in water or PEG solutions. Specifically, the dynamic technique enables measurement of the viscosity, μ, of the intervening fluid as a function of surface separation. The method involves vibrating the upper surface by applying an ac voltage to the piezoelectric crystal that results in a normal oscillation of the upper surface at a frequency ν and amplitude A_0. The viscous coupling of the upper and lower surface due to the liquid between the surfaces induces the lower surface, supported by a double cantilever with spring constant K, to vibrate at the same frequency ν but with an amplitude A_x. If the amplitude A_0 and the frequency ν of the upper surface remain fixed, but the mean separation $\bar{D}$ is reduced, the viscous force on the lower surface increases. Thus, as the two surfaces approach each other their separation will oscillate with decreasing amplitude $A = A_0 - A_x$, where $A \rightarrow A_0$ for large $\bar{D}$, and $A \rightarrow 0$ as $\bar{D} \rightarrow 0$. For low amplitudes and low frequencies, i.e., low shear rates, where fluid inertial and acceleration terms can be ignored and the only opposition to flow is due to the fluid viscosity, the mean gap viscosity can be calculated from

$$\mu = \frac{K\bar{D}}{12\pi^2 R^2 \nu}\left[(A_0/A)^2 - \left(1 - \frac{f}{K}\right)^2\right]^{1/2} \quad (1)$$

where $\bar{D}$ is the mean separation during the oscillation, R is the effective hydrodynamic radius of the curved surfaces, and f is the gradient of the static force at $\bar{D}$.[21]

Whereas eq 1 gives an average viscosity of all of the fluid in the gap, more information about local viscosities can be derived from a plot of

$$12\pi^2 R^2 \nu K^{-1}[(A_0/A)^2 - (1 - f/K)^2]^{1/2} \quad (2)$$

vs $\bar{D}$. From such a plot, the inverse slope of the chord (the line from the origin to the data point) gives the average viscosity of the fluid in the whole gap, while the inverse slope of the curve at the data point gives the local viscosity of the film at the midpoint between the surfaces at any given surface separation $\bar{D}$. In addition, the x-axis intercept of the line—extrapolated back from large separations—gives the effective location of the shear plane for the measurements. For nonideal systems where the shear plane is not at the surfaces due to an adsorbed, immobile film, or where a depletion layer modifies the flow in the gap, more information can be extracted from this type of plot.

Results and Discussion

Static Force Measurements. General Overview. Figure 2 gives a general overview of the normal force profiles measured between lipid bilayers in water as well as in aqueous solutions of PEG 8k.[13] All measurements were made at 25 °C. In the absence of polymer (dotted curve, Figure 2), the neutral lipid bilayers weakly adhere to each other via a van der Waals interaction with an energy minimum of −0.5 mN/m,

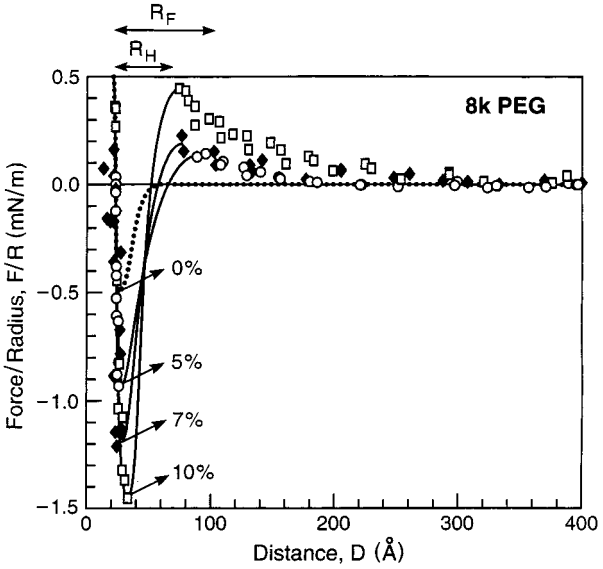

Figure 2. Force profiles, F/R vs D, between supported DPPE/DMPC bilayers in water and aqueous 8k PEG solutions. The dashed curve is the force profile in water, i.e., in the absence of polymer, where the bilayers adhere due to van der Waals attraction. The bilayers are prevented from approaching closer than $D \approx 20$ Å by the strong short-range steric−hydration repulsion. The arrows indicate when the spring constant is exceeded by the gradient in the attractive force. The resulting mechanical instability causes the surfaces to jump together or apart. Thus, these portions of the force profile are inaccessible.

separations below $D \approx 20$ Å are opposed by strong repulsive hydration and steric protrusion forces.[17] In the presence of 8k MW PEG at 5−10 wt %, the measured hard wall of bilayer−bilayer contact occurs at the same separation (∼20 Å), but the adhesive minimum is significantly greater than the always present van der Waals attraction. As we will show, the increased adhesion is due to a depletion attraction interaction in the presence of nonadsorbing polymer chains. However, there is also an unexpected repulsive force at larger separations ($D \sim 300$ or $4R_F$) prior to the attractive regime.

Source of the Repulsion Measured in the Presence of 8k PEG. In a recent series of experiments utilizing dynamic light scattering, Porsch and Sundelöf[14] examined whether PEG forms aggregates in water. By comparing the scattering autocorrelation functions before and after filtering the PEG samples through 0.02−0.8 μm filters, they concluded that PEG itself does not aggregate in dilute water solutions. Moreover, using size exclusion chromatography, they determined that the large scattering bodies, previously thought to be PEG aggregates, were indeed aggregates but nucleated by hydrophobic impurities. PEG is known to be an extremely good particle stabilizer and effectively coated these impurity particles, i.e., sterically stabilized them in solution. Commercial grade PEG 20k from Fluka (which is the same chemically as the 20k from Polysciences used in our studies in part 2 of this work) was investigated as well as high purity monodisperse PEG samples.

Following the same protocol outlined by Porsch and Sundelöf, we filtered a PEG 8k 10 wt % solution through a 0.02 μm Anodisc alumina matrix membrane filter. The force profiles measured immediately (20−50 min) after mounting the bilayer-coated mica surfaces in the SFA

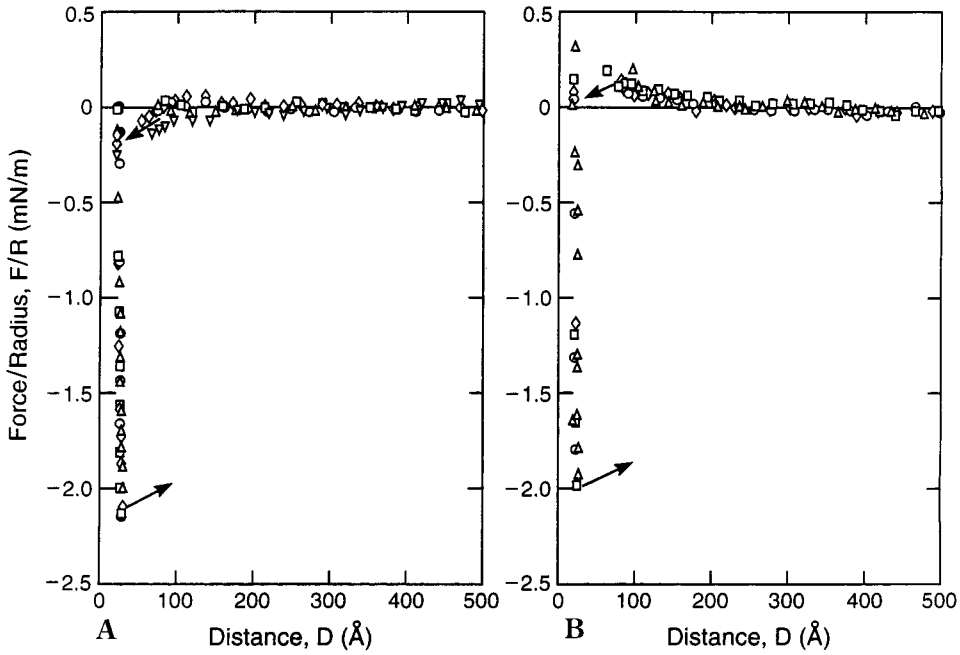

Figure 3. (A) Force profiles with filtered 10 wt % PEG 8k solutions measured within 1 h of mounting the bilayer coated mica surfaces into the SFA. No repulsion is detected prior to the jump into a depletion attraction enhanced minimum. (B) Repulsive barrier in filtered 10 wt % PEG 8k solutions that develops with time (3 h).

were purely attractive; i.e., no repulsion was measured (Figure 3A). The jumps into bilayer−bilayer contact were also very rapid. The magnitude of the adhesion was significantly greater, $F_a/R = 2.1$ mN/m vs 1.6 mN/m in the unfiltered case. (Note, the *difference* is almost exactly the magnitude of the repulsive force barrier measured with the unfiltered solutions, Figure 2.) After waiting an additional 2 h, the force profiles became weakly repulsive prior to the attractive regime, becoming more similar to the force profiles obtained with unfiltered PEG 8k 10 wt % (Figure 3B). Although the magnitude of the repulsion was less than that with unfiltered solutions, the range of the repulsion was about the same. Additionally, the repulsive regime of the force profile was reversible; i.e., no hysteresis in the magnitude or range of the repulsive force was detected when comparing the approach to the separation. Another interesting aspect is that the adhesion decreased from 2.1 to 1.9 mN/m as the repulsive barrier magnitude increased from 0 to 0.2 mN/m; again, the differences are equal. These findings suggest that the attractive and repulsive forces are additive, i.e., they have different origins. Finally, the jumps into contact were more rapid with the filtered solutions, while the jump rate decreased once a repulsive barrier was present.

Attractive Depletion Interaction and the Repulsive Barrier. If the enhanced adhesion found in the presence of PEG 8k is due to depletion attraction, its magnitude should correspond to the bulk osmotic pressure. At a concentration of 10 wt % PEG 8k, the magnitude of the adhesion decreases from a high value of 2.15, to 1.9, and finally to 1.6 mN/m as the repulsion increases from 0 (initial filtered solutions) to 0.2 (later filtered solutions) to almost 0.5 mN/m in the unfiltered case, respectively.[1] Essentially, the difference between the repulsive barriers and the adhesion forces at "contact" is constant in all experiments and equal to $F_{total}/R = 2.1$ mN/m. After subtracting the van der Waals contribution to the attraction ($F_{vdW}/R \approx 0.5$ mN/m, Figure 2), the remaining adhesive force is about 1.6 mN/m. This is consistent with the expected additivity of the van der Waals attraction and depletion interaction. Moreover, the adhesion at contact in the absence of any repulsion should be only due to the attractive van der Waals and depletion interaction (Figure 3A). Thus, a value of $F_a/R = 1.65 \pm 0.1$ mN/m should correspond to the osmotic pressure of bulk PEG 8k solution at 10 wt %. The literature value for the bulk osmotic pressure, which is highly nonideal, was obtained from the polynomial derived by Michel and co-workers,[23] who fitted the osmotic pressure of PEG 8k over a large range of temperatures and concentrations to obtain

$$\Pi(atm) = 1.29TG^2 + 140G^2 + 4G \qquad (3)$$

where G is the weight percent polymer and T is the temperature in °C.[29]

The experimentally measured adhesion force between two cylindrical surfaces, F/R, can be readily compared to the osmotic pressure, Π, using the Derjaguin approximation:[24]

$$\Pi = \frac{\partial E(D)}{\partial D} = \frac{1}{2\pi R}\frac{\partial F(D)}{\partial D} \qquad (4)$$

Using self-consistent mean field theory, Vincent et al.[3] and more recently Evans[12] found that the depletion force had essentially a linear distance dependence for separations less than twice the depletion layer thickness, $D \leq 2\Delta$, where Δ is the correlation length of a polymer coil in solution.[25] Therefore, at small separations we have assumed a linear distance dependence on the depletion energy:

$$E(D) = (D - 2\Delta)\Pi, \quad D < 2\Delta \qquad (5)$$

Using eqs 4 and 5, the experimental results in Figures 2 and 3A, B can be converted to bulk osmotic pressure. In other words, the slope of the force (divided by 2π) over the distance at which the surfaces jump in to and

Table 1[a]

8k PEG wt %[29]	bulk osmotic pressure (atm), eq 3	experimental osmotic pressure (atm), eq 5
5	0.38	0.40 ± 0.2
7	0.64	0.58 ± 0.2
10	1.23	1.09 ± 0.2

[a] As we will show in the following paper, part 2, this weak repulsion is most likely an electrostatic force due to chelation of metal cations.

out of contact is the osmotic pressure. Using polymer scaling theory, we calculate $\Delta = 14$ Å.[25] The effective depletion layer thickness, 2Δ, from the data in Figure 3A is 25 ± 5 Å, which matches well to the theorectical value. Using this length scale, the experimentally determined osmotic pressure is $\Pi_{exp} = 1.1 \pm 0.2$ atm, which agrees nicely with the bulk osmotic pressure, $\Pi = 1.2$ atm, derived using eq 3. Table 1 provides a comparison of the concentration dependence of the measured adhesion versus the calculated bulk osmotic pressure for PEG 8k concentrations of 5, 7, and 10 wt %.[13] As can be seen, the experimental measurements are in very good agreement with the bulk osmotic pressures for those polymer concentrations.

At this point, we will leave the resolution of the source of the repulsive barrier until part 2 of this work. The behavior as the MW of the PEG chains increases is very informative and enables one to resolve all aspects of these interesting direct force measurements.

Dynamic Viscosity Measurements. Water Viscosity. The issue of whether water structures at surfaces has been debated since the early 1900s and remains controversial.[26] Lyklema and co-workers resolved some aspects of this issue regarding water structuring at lipid surfaces in 1964.[27] By studying the flow or drainage of water between two surfactant monolayers (the thinning of a soap film), they concluded that the viscosity of water, extrapolated from data on films greater than 400 Å thick, remains that of the bulk within the accuracy of their measurements, i.e., within 10 Å of each surface. Hence, there were no rigidified water layers near the surfactant headgroups or water structure extending out from the surface over the time scales of their measurements. However, this is not to say that the headgroups are not "hydrated", just that no change in water viscosity due to "water structuring" was detected in their measurements.

Our dynamic measurements of the viscosity of water between two bilayer coated surfaces are complementary to those measurements made 30 years earlier by Lyklema and co-workers. As shown in Figures 4 and 5, we too do not detect any increase in the viscosity of water down to separations of 60 Å (smaller separations were not experimentally accessible). As in our previous figures, the distance reference frame, $D = 0$, is based on the chemical structure of dehydrated DMPC, i.e., dehydrated lipids which do not protrude from the membrane surface (Figure 1). Hence, the bilayers are in contact at $D = 20$ Å (Figure 2). Using the same reference for distance, Marra and Israelachvili[18] determined that the van der Waals plane for DMPC monolayers was at about $D = 11$ Å or 5.5 Å per surface. In our dynamic measurements, we find the shear plane to be at $D = 8 \pm 7.5$ Å per surface. This is consistent with a single monolayer of water "bound" on each surface ($D_{shear} - D_{vdw} = 2\delta = 5$ Å, or $\delta = 2.5$ Å). Note, the measured bulk viscosity of 1.0 ± 0.1cP for all separations is slightly higher than the literature value for water, $\mu = 0.9$ cP, due to most likely a small error in the radius of curvature measurement (cf. eq 1).[28] Thus, no long-range water structuring from the bilayer surface is detected. This result suggests that "hydration" repulsion is considerably smaller than protrusion repulsion and acts by pushing out the position of contact by one immobilized layer of water per surface. In a self-consistent manner, we use the same reference frame of $D_{origin} = 16$ Å (8 Å per surface) for the shear plane in the analysis of the viscosity profiles in PEG solutions.

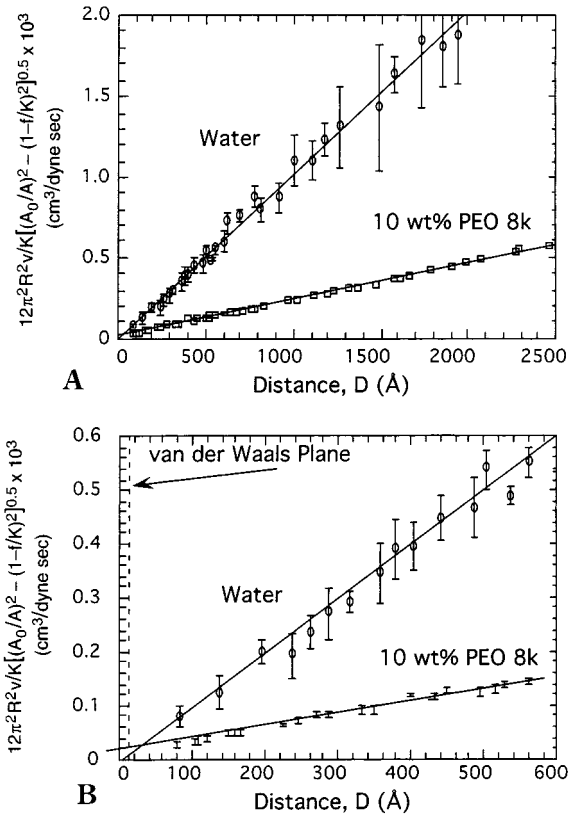

Figure 4. (A) Plot of $(12\pi^2R^2\nu)/(K)[(A_0/A)^2 - (1 - f/K)^2]^{1/2}$ against distance D for water and 10 wt % PEG 8k at 25 °C. Ideally, if the viscosity equals the bulk value at all distances, the points should fall on a straight line whose inverse slope gives the viscosity. The intercept of the line with the D axis, occurs at the plane of shear. The error bars are the standard deviation for each measurement. Note, the error becomes less at smaller separations. In addition, the higher bulk viscosities in the presence of polymer enhance the accuracy of those measurements. The shear plane between two bilayers in water is located at $D = +16$ Å. Compared to the origin of the van der Waals plane at $D = 11$ Å, this is consistent with a single layer of water molecules bound to each bilayer surface. At large separations, the effective shear plane in 10 wt % PEG 8k is located at $D = -60$ Å, while at smaller separations the shear plane shifts to less negative values approaching the same position as found in pure water; i.e., in the absence of polymer. This effect can be fully explained by the presence of a lower viscosity solution near the bilayer surfaces. (B) Same as part A but in more detail.

PEG 8k at 10 wt % Viscosity. The dynamic viscosity measurements with the PEG 8k solution between the bilayers are complimentary to the static force measurements and provide more information about the depletion effect. At separations greater than 1000 Å, the viscosity in the gap is that of the bulk polymer solution, 4.3 cP (see parts A and B of Figure 5).[30] With decreasing separation the average gap

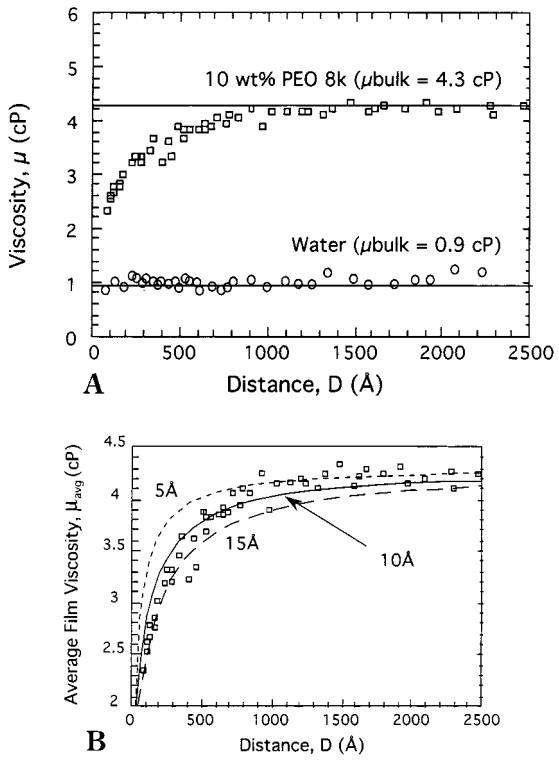

Figure 5. (A) Viscosity as a function of distance calculated using eq 1. No change in the viscosity of water is detected. Conversely, the viscosity decreases significantly as a function of separation when the free polymer chains are depleted from the region near the surface in PEG 8k at 10 wt %. (B) Theoretical calculations of the viscosity in solutions of PEG 8k at 10 wt %. The symbols are the experimental data and the solid and dashed lines are theoretical calculations using different depletion layer thicknesses in the model and equations detailed in the Appendix. The best fit to the experimental data is obtained for a fixed depletion layer thickness of 10 Å per surface.

viscosity drops monotonically to 2.2 cP at 80 Å (using the chord measurement), which is significantly less than that of the bulk solution but higher than the value for pure water. The *effective* shear plane, as taken from the *x*-intercept in Figure 4B, is negative for this system, which is indicative of a lower viscosity solution near the bilayer surfaces. Extrapolating from large separations we find that $D_{shear} = -60$ Å. However, fitting points at separations less than 350 Å leads to $D_{shear} = -37$ Å, and below 200 Å to $D_{shear} = -20$ Å. These calculations of *effective* shear planes at negative distances can be quantitatively explained by a low viscosity depletion layer near the bilayer surfaces.[31] At large separations, the thin depletion layers contribute minimally to the local viscosity of the fluid at the midpoint between the surfaces, resulting in an accurate measurement of the bulk viscosity. However, their presence is directly reflected by the large negative effective shear planes. At smaller separations, however, the shear stress at the surfaces increases and flow in the depletion layer has a greater impact on the measured solution viscosity, reducing its mean value.

In an effort to quantify the depletion effect on the measured fluid flow characteristics, the Navier−Stokes equations that were used to derive eq 1 were used to rederive the flow profiles for the case of a layer of lower viscosity solution (depletion layer) near the bilayer surfaces (see Appendix). Using similar assumptions as Israelachvili and co-workers,[21] the viscous drag coefficient g was calculated as a function of separation for a thin depletion layer of viscosity $\mu = 0.9$ cP (equivalent to polymer-free water) at each surface. The sole adjustable parameter for the fit to the experimental data was the depleted layer thickness, which was varied from 0 to 20 Å per surface. Figure 5B shows the calculated gap viscosity as a function of surface separation for different depletion layer thicknesses. The experimental data is well fit by this model with a fixed depletion layer of 10 Å per surface. The theoretical depletion layer thickness of 10 Å also agrees very well with the experimentally determined thickness of 13 Å (or 25 ± 5 Å for two surfaces, Figure 3A). Donath and coworkers obtained similar results in their astute studies of the electrophoretic mobility of liposomes in dextran solutions.[31]

At very small separations ($D < 2\delta$, which is beyond the experimental capabilities), the data should still reflect the presence of polymer between the surfaces at larger radial distances. This explains why the viscosity never falls to 0.9 cP, even at the smallest separations in the calculation.

In summary, the viscosity measurements are consistent with the force measurements and further demonstrate the presence of a thin depletion layer near each of the bilayers that significantly affects the flow of polymer solution between the surfaces.

Conclusions

Depletion attraction due to a nonadsorbing polymer has been directly measured utilizing both static force measurements and dynamic, thin film viscosity measurements. The additional adhesion measured between the surfaces in solutions of PEG 8k corresponded directly to the bulk osmotic pressure of the polymer solution. However, the thin film viscosity measurements were particularly sensitive to the polymer-depleted region adjacent to the surface. In addition, the viscosity of water confined between two bilayer surfaces is the same as that of the bulk. The shear plane is located 3 Å farther out than the van der Waals plane per bilayer surface, consistent with one, effectively immobilized, layer of water molecules per lipid surface.

Acknowledgment. We thank Phil Pincus for helpful discussions and for pointing out the possibility of PEG aggregates in solution, Dave Jordan of PolySciences for graciously answering many questions on the chemistry of PEG; Stefan Bekiranov for the PEG 20k chemical structure, and Mike Lyon for assistance in measuring the bulk solution viscosities. This work was supported by NIH Grants GM 47334 and GM 30969.

Appendix

The radial component of the Navier−Stokes equation of motion in cylindrical coordinates assuming constant viscosity μ and density ρ, neglecting acceleration terms is

$$\frac{\partial P}{\partial r} = \mu\left[\frac{\partial}{\partial r}\left(\frac{1}{r}\frac{\partial}{\partial r}(r v_r)\right) + \frac{\partial^2 v_r}{\partial z^2}\right] - \rho\left[v_r\frac{\partial v_r}{\partial r} + v_z\frac{\partial v_r}{\partial z}\right] \quad \text{(A1)}$$

where P is the scalar pressure at radial coordinate r, and v is the fluid velocity in the subscripted direction. The system to be modeled is dissected into two parts: a thin depletion layer of thickness δ and viscosity μ^{δ} at each surface, and the main bulk polymer solution of viscosity μ^{b} occupying the remainder of the gap between

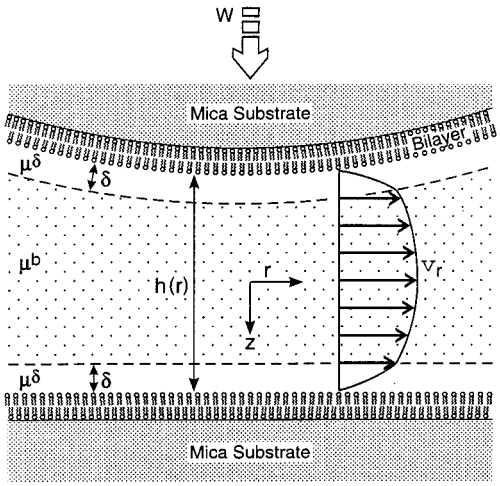

Figure 6. Schematic showing how the system is modeled. A thin depletion layer of thickness δ and viscosity μ^δ is adjacent to the bilayer surface, and the main bulk polymer solution of viscosity μ^b occupies the remainder of the gap between the surfaces. Because of the relatively large radius of curvature R, the velocity profile within each layer can be assumed to be parabolic.

the surfaces (see Figure 6). Due to the relatively large radius of curvature R of the surfaces, the velocity profile within each layer can be assumed to be parabolic. Using no-slip boundary conditions at all of the interfaces, and constant stress at the depletion layer/bulk interface, velocity profiles within each layer in terms of the radial pressure gradient were determined:

$$v^b = \frac{1}{2\mu^b}\frac{\partial P}{\partial r}z^2 + \frac{1}{2}\frac{\partial P}{\partial r}\left(\frac{\delta^2 - h\delta}{\mu^\delta} - \frac{(h/2-\delta)^2}{\mu^b}\right) \quad \text{(A2)}$$

$$v^\delta = \frac{1}{2\mu^\delta}\frac{\partial P}{\partial r}z^2 - \frac{h^2}{8\mu^\delta}\frac{\partial P}{\partial r}$$

where $h \approx h_0 + r^2/2R$ is the distance between the surfaces. The pressure profile $P(r)$ can be solved from eq A2 using the continuity equation

$$P(r') = -\int_\infty^{r'} \mathrm{d}r \frac{wr}{4}\left\{(h/2-\delta)\left[\frac{1}{6\mu^b}(h/2-\delta)^2 + \frac{1}{2}\left(\frac{\delta^2 - h\delta}{\mu^\delta} - \frac{(h/2-\delta)^2}{\mu^b}\right)\right] + \frac{1}{6\mu^\delta}\left[\frac{h^3}{8} - (h/2-\delta)^3\right] + \frac{h^2\delta}{8\mu^\delta}\right\}^{-1} \quad \text{(A3)}$$

where w is the velocity that the surfaces approach each other. The net force between the surfaces comes from integrating the pressure over the surface area:

$$F = \int_0^\infty \mathrm{d}r' \, 2\pi r' P(r') \quad \text{(A4)}$$

The integral was calculated numerically as a function of surface separation for different depletion layer thicknesses. These results were interpreted in terms of an effective viscosity of the composite fluid between the surfaces, and were compared to the experimental data in Figure 5B.

References and Notes

(1) Asakura, S.; Oosawa, F. *J. Chem. Phys.* **1954**, *22*, 1255−1256. Asakura, S.; Oosawa, F. *J. Polym. Sci.* **1958**, *33*, 183−192.

(2) Joanny, J. F.; Leibler, L.; de Gennes, P. G. *J. Polym. Sci.: Polym. Phys. Ed.* **1979**, *17*, 1073. Vrij, A. *Pure Appl. Chem.* **1976**, *48*, 471−483. de Gennes, P. G. *Macromolecules* **1981**, *14*, 1637−1644. Fleer, G.; Scheutjens, J. In *Polymer Adsorption and Dispersion Stability*; Goddord, E. B., Vincent, B., Eds.; American Chemical Society: Washington, DC, 1984; p 245. Woodward, C. E. *J. Chem. Phys.* **1992**, *97*, 695−702. For a nice review, see: Yethiraj, A.; Hall, C. K.; Dickman, R. *J. Coll. Inter. Sci. 151*, 102−117.

(3) Fleer, G. J.; Scheutjens, J. H. M. H.; Vincent, B. In *Polymer Adsorption and Dispersion Stability*; Goddord, E., Vincent, B., Eds.; ACS Symposium Series; American Chemical Society: Washington, DC, 1984; pp 245−263. They also found a demixing energy barrier prior to the attractive regime. However, the magnitude of the repulsion was negligibly small.

(4) Feigin, R.; Napper, D. *J. Colloid Interface Sci.* **1980**, *74*, 567. Feigin, R.; Napper, D. *J. Colloid Interface Sci.* **1980**, *75*, 525.

(5) Walz, J. Y.; Sharma, A. *J. Colloid Interface Sci.* **1994**, *168*, 485−496.

(6) Mao, Y.; Cates, M. E.; Lekkerkerker, H. N. W. *Physica A* **1995**, *222*, 10−24. Mao, Y.; Cates, M. E.; Lekkerkerker, H. N. W. *Phys. Rev. Lett.* **1995**, *75*, 4548−4551. Mao, Y. *J. Phys. II* **1995**, *5*, 1761−1766.

(7) Richetti, R.; Kekicheff, P. *Phys. Rev. Lett.* **1992**, *68*, 1951−1954. Parker, J. L.; Richetti, P.; Kekicheff, P.; Sarman, S. *Phys. Rev. Lett.* **1992**, *68*, 1955−1958.

(8) Sober, D. L.; Walz, J. Y. *Langmuir* **1995**, *11*, 2352−2356.

(9) Perez, E.; Proust, J. E. *J. Phys. Lett* **1985**, *46*, L79−L84.

(10) Arnold, K.; Pratsch, L.; Gawrisch, K. *Biochim. Biophys. Acta* **1983**, *728*, 121. Arnold, K.; Hermann, A.; Gawrisch, K.; Pratsch, L. *Stud. Biophys.* **1985**, *110*, 135.

(11) Arnold, K.; Lvov, Y. M.; Szogyi, M.; Gyorgyi, S. *Stud. Biophys.* **1986**, *113*, 7. Arnold, K.; Zschoernig, O.; Barthel, D.; Herold, W. *Biochim. Biophys. Acta* **1990**, *1022*, 303.

(12) Evans, E.; Needham, D. In *Molecular Mechanisms of Membrane Fusion*; Ohki, S., Doyle, D., Flanagan, T. D., Hui, S. W., Mayhew, E., Eds.; Plenum Press: New York, 1988; p 83. Evans, E.; Needham, D. *Macromolecules* **1988**, *21*, 1822−1831. Evans, E. *Macromolecules* **1989**, *22*, 2277−2286.

(13) Kuhl, T. L.; Guo, Y.; Alderfer, J. L.; Berman, A. D.; Leckband, D. Israelachvili, J. N.; Hui, S. W. *Langmuir* **1996**, *12*, 3003−3014.

(14) Porsch, B.; Sundelöf, L.-O. *Macromolecules* **1995**, *28*, 7165−7170.

(15) Bekiranov, S.; Bruinsma, R.; Pincus, P. *Phys. Rev. E* **1997**, *55*, 577−585.

(16) Israelachvili, J. *J. Colloid Interface Sci.* **1973**, *44*, 259. Israelachvili, J.; Adams, G. *Nature (London)* **1976**, *262*, 774.

(17) Blow, A. M. J.; Botham, G. M.; Fisher, D.; Goodall, A. H.; Tilcock, C. P.; Lucy, J. A. *FEBS Lett.* **1978**, *94*, 305. Tilcock, D. P. S.; Fisher, D. *Biochim. Biophys. Acta* **1982**, *688*, 645. Boni, L. T.; Hah, J. S.; Hui, S. W.; Mukherjee, P.; Ho, J. T.; Jung, C. Y. *Biochim. Biophys. Acta* **1984**, *775*, 409. Boni, L. T.; Hui, S. W. In *Cell Fusion*; Sowers, A., Ed.; Pluenum Press: New York, 1987; p 301. Arnold, K.; Hermann, A.; Pratsch, L.; Gawrisch, K. *Biochim. Biophys. Acta* **1985**, *815*, 515.

(18) Marra, J.; Israelachvili, J. *Biochemistry* **1985**, *24*, 4608.

(19) Tanford, C. *J. Phys. Chem.* **1972**, *93*, 917.

(20) Small, D. M. *J. Lipid Res.* **1967**, *8*, 551.

(21) Israelachvili, J. N. *J. Colloid Interface Sci.* **1986**, *110*, 263−271. Israelachvili, J. N.; Kott, S. J. *J. Colloid Interface Sci.* **1989**, *129*, 461−467.

(22) In all of the experiments described in this work, the outer DMPC monolayers could always be completely removed from the DPPE−mica surface. To do this, the aqueous solution was drained from the SFA, when the bilayers went through the air−water interface, the outer DMPC monolayers were removed. When the surfaces were brought together, strong hydrophobic contact of the two remaining DPPE layers was always obtained. This feature indicates that the integrity of both the inner and outer monolayers of the bilayer were always maintained even in the presence of high concentrations of polymer or polymer adsorption to the DMPC surface.

(23) Michel, B. E.; Kaufmann, M. R. *Plant Physiol.* **1973**, *51*, 914−916. Parsegian, V. A.; Rand, R. P.; Fuller, N. L.; Rau, D. C. In *Methods in Enzymology*, Packer, L., Ed.; Academic Press: Orlando, FL, 1986; Vol. 127, pp 400−416.

(24) Derjaguin, B. V. *Kolloid Z.* **1934**, *69*, 155−164.

(25) Vincent, B.; Luckham, P. F.; Waite, F. A. *J. Colloid Interface Sci.* **1980**, *73*, 508. Rao, I. V.; Ruckenstein, E. *J. Colloid*

Interface Sci. **1985**, *108*, 389. Vincent, B.; Edwards, J.; Emmet, S.; Jones, A. *Colloids Surf.* **1986**, *18*, 261. Van Lent, B.; Scheutjens, J. M. H. M.; Fleer, G. J. *J. Colloid Interface Sci.* **1990**, *137*, 380−394. Wijmans, C. M.; Zhulina, E. B.; Fleer, G. J. *Macromolecules* **1994**, *27*, 3238−3248.

(26) Rand, R. P.; Parsegian, V. A. *Biochim. Biophys. Acta*. **1989**, *988*, 351−376. McIntosh, T. J.; Simon, S. A. *Annu. Rev. Biophys. Biomol. Struct.* **1994**, *23*, 27−51. Israelachvili, J.; Wennerström, H. *Nature* **1996**, *379*, 219−225.

(27) Lyklema, J.; Scholten, P. C.; Mysels, K. J. *J. Phys. Chem*. **1965**, *69*, 116−123. See also: Haydon, D. A. *Proc. R. Soc. A* **1960**, *258*, 319−328. Carroll, B. J.; Haydon, D. A. *Proc. R. Soc. A* **1974**, 361−377.

(28) *Handbook of Chemistry and Physics*; CRC Press: Boca Raton, FL, 1990.

(29) The actual polymer concentration in weight percent is approximately 12% lower than the listed value due to unavoidable dilution during the installation of the bilayer coated surfaces into the SFA.

(30) Bulk viscosity measurements were made with unfiltered polymer solutions.

(31) Krabi, A.; Donath, E. *Colloids Surf., A: Physicochem. Eng. Aspects* **1994**, *92*, 175. Donath, E.; Krabi, A.; Allan, G.; Vincent, B. *Langmuir* **1996**, *12*, 3425−3430.

(32) Ogden, A. L.; Lewis, J. A. *Langmuir* **1996**, *12*, 3413−3424.

MA971431D